

Tuning singlet fission in tetracene nanoparticles by controlling molecular packing with side-group engineering

Zhaofeng Tang, Sainan Zhou, Heyuan Liu,* Xiangyang Wang, Shanshan Liu, LiShen,
Xiaoqing Lu and Xiyu Li*

Content

1. SEM images of DPhTc-(COOH)₂ NP	2
2. XRD patterns of nanoparticles and drop-casting films for DPhTc, DPhTc-COOH and DPhTc-(COOH)₂	3
3. The most stable geometry optimized structures of DPhTc-COOH without and with water molecules	4
4. The fluorescence dynamics of these three nanoparticles probed at different wavelengths	5
5. Triplet sensitization experiment	7
6. Comparison of TA spectra between the raw data and the fitting data	12
7. Singular value decomposition of <i>ns</i>-TA	15
8. Triplet yield determination	16
9. Comparison of the arrangement between the minimized packing of DPhTc nanoparticle and its crystal	19
10. Simulation of the packing structure of these molecules at the interface of air/water	23
11. Calculation of the splitting energy of the singlet state	25
12. ¹H NMR and MALDI-TOF spectra of new compounds	28
REFERENCES	34

1. SEM images of DPhTc-(COOH)₂ NP

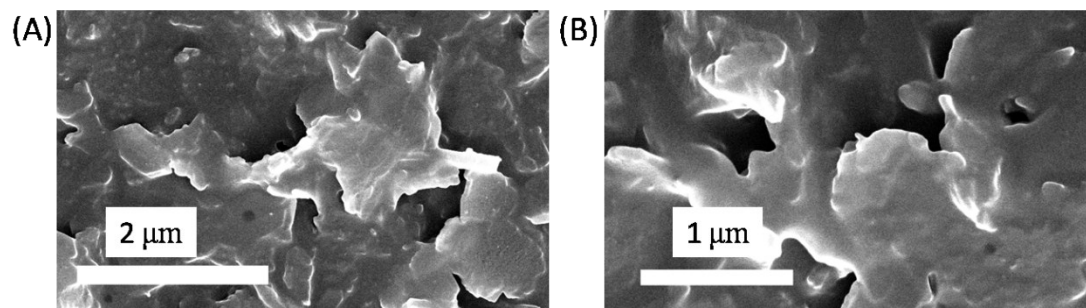


Fig. S1 SEM images of DPhTc-(COOH)₂.

2. XRD patterns of nanoparticles and drop-casting films for DPhTc, DPhTc-COOH and DPhTc-(COOH)₂

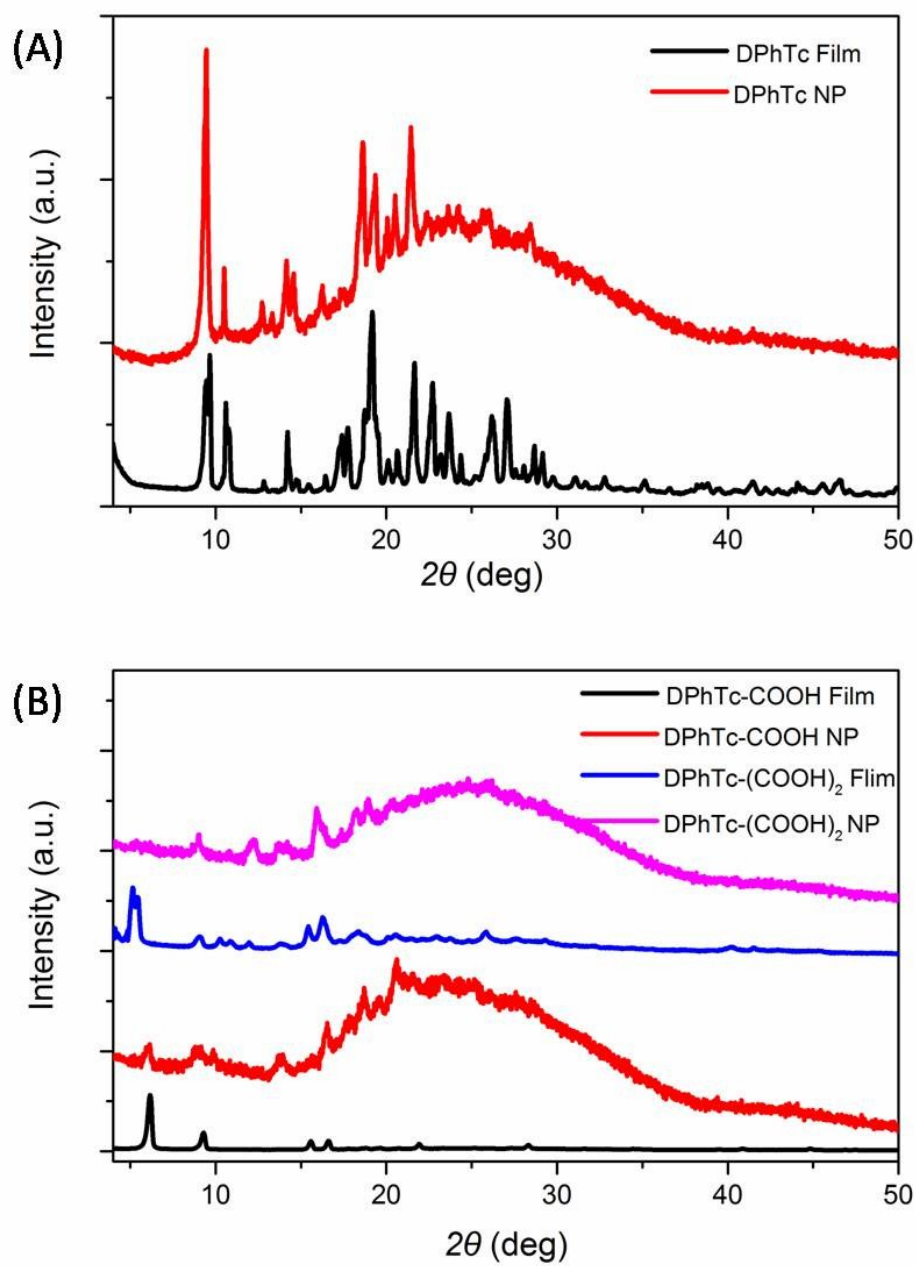


Fig. S2 XRD patterns of nanoparticles and drop-casting films for DPhTc (A), DPhTc-COOH (B) and DPhTc-(COOH)₂ (B).

3. The most stable geometry optimized structures of DPhTc-COOH without and with water molecules

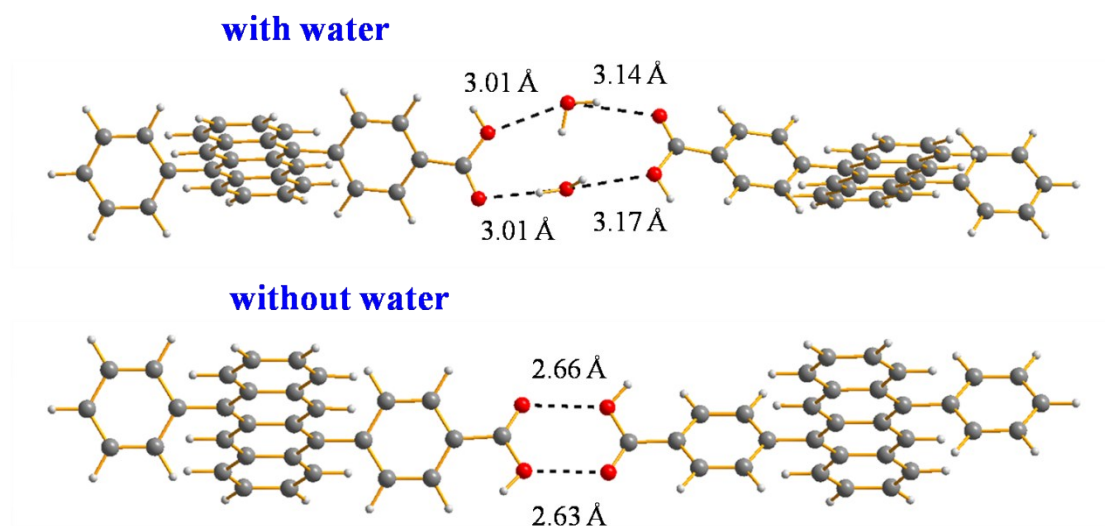


Fig. S3 The most stable geometry optimized dimeric structures of DPhTc-COOH without and with water molecules. The hydrogen bonds length was also shown.

4. The fluorescence dynamics of these three nanoparticles probed at different wavelengths

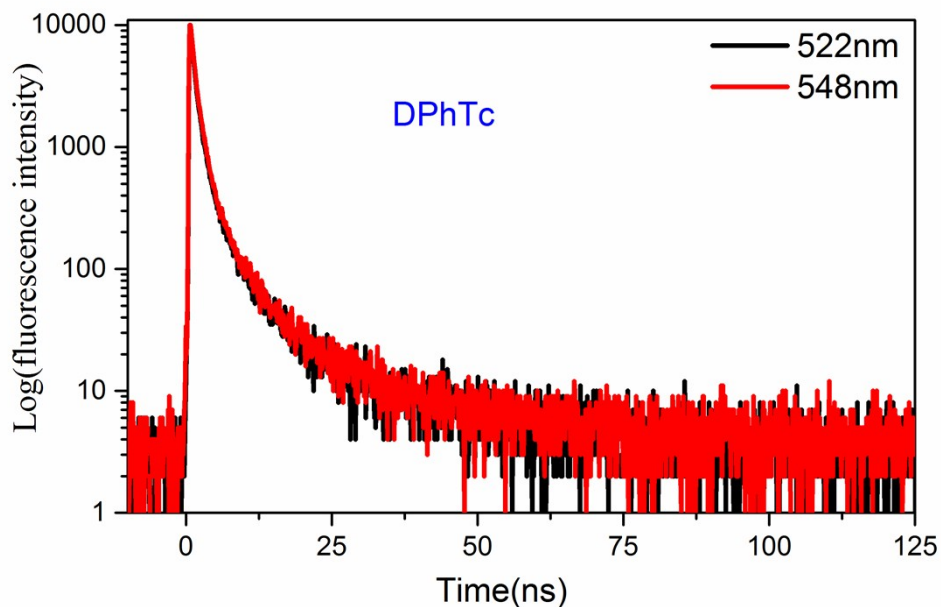


Fig. S4 The fluorescence dynamics of DPhTc nanoparticle probed at different wavelengths (excited at 441 nm).

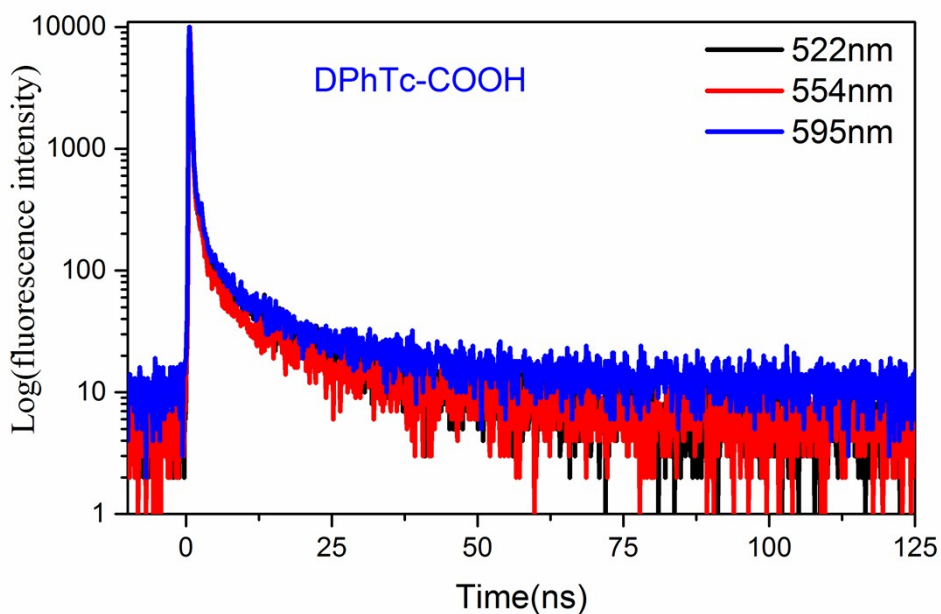


Fig. S5 The fluorescence dynamics of DPhTc-COOH nanoparticle probed at different wavelengths (excited at 441 nm).

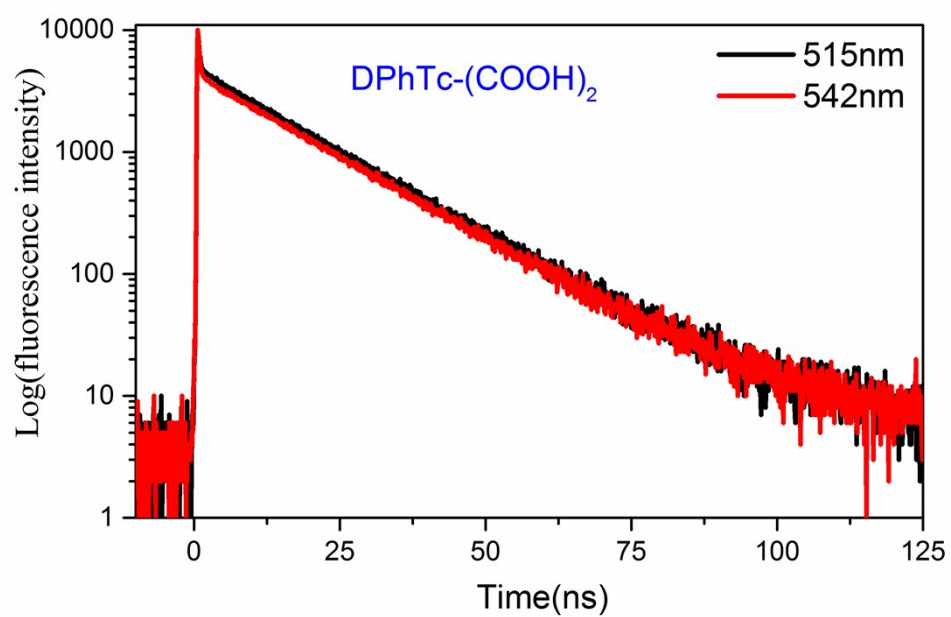


Fig. S6 The fluorescence dynamics of DPhTc-(COOH)₂ nanoparticle probed at different wavelengths (excited at 441 nm).

5. Triplet sensitization experiment

To obtain the triplet spectral signature of DPhTc, DPhTc-COOH and DPhTc-(COOH)₂ NPs, triplet sensitization of DPhTc, DPhTc-COOH and DPhTc-(COOH)₂ suspensions was performed with the known triplet sensitizer, PdTPTBP. The triplet sensitization NP sample were prepared by adding 0.4 mL THF solution of 0.380 mg of DPhTc, 0.424 mg of DPhTc-COOH or 0.469 mg of DPhTc-(COOH)₂ and 0.01 mg of PdTPTBP to a vigorously stirred deionized water (10 mL). For comparison, PdTPTBP NP was also prepared by re-precipitation method as mentioned in the text. All the samples is prepared in glovebox and all the solvents are degassed first by Freeze-Pump-Thaw method. Selective photoexcitation of the PdTPTBP at 630 nm results in rapid intersystem crossing followed by triplet energy transfer to DPhTc, DPhTc-COOH or DPhTc-(COOH)₂ (Fig. S8-S10). At initial times, the clear spectral signature corresponding to the reported T₁-T_n absorption (550 nm) and the ground-state bleaching (GSB) (440-460nm) of PdTPTBP (Fig. S7-S10) were observed.^{1,2} As the time increased, the triplet absorption of PdTPTBP centered at 550 nm decayed almost completely in hundred picoseconds (Fig. S8B-S10B). Meanwhile, the GSB band of PdTPTBP was also decreased significantly. A new spectrum with the main absorption band at 485-525 nm emerges, which can be assigned to the T₁ state of phenyl substituted tetracene based on the previous report.³⁻⁵

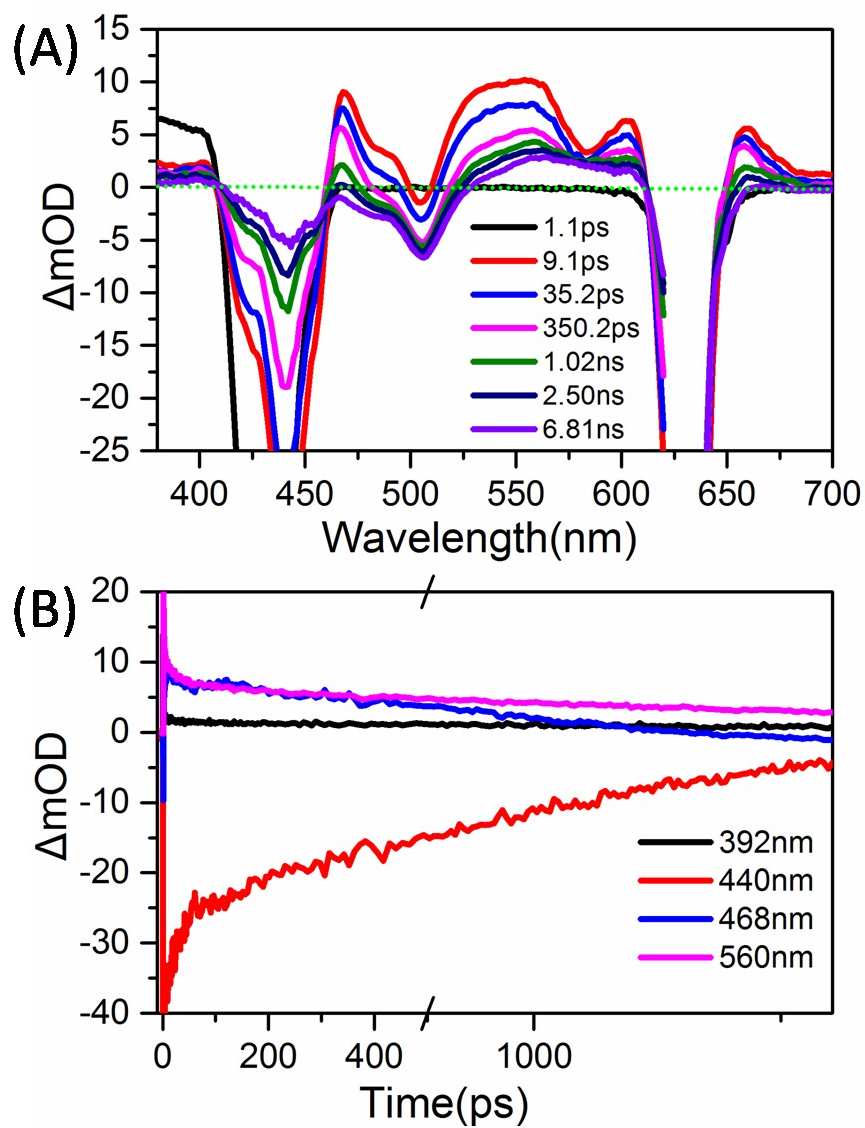


Fig. S7 (A) TA spectra of PdTPTBP NP following excitation at 630 nm. (B) Single-wavelength dynamics of PdTPTBP NP probed at different wavelengths.

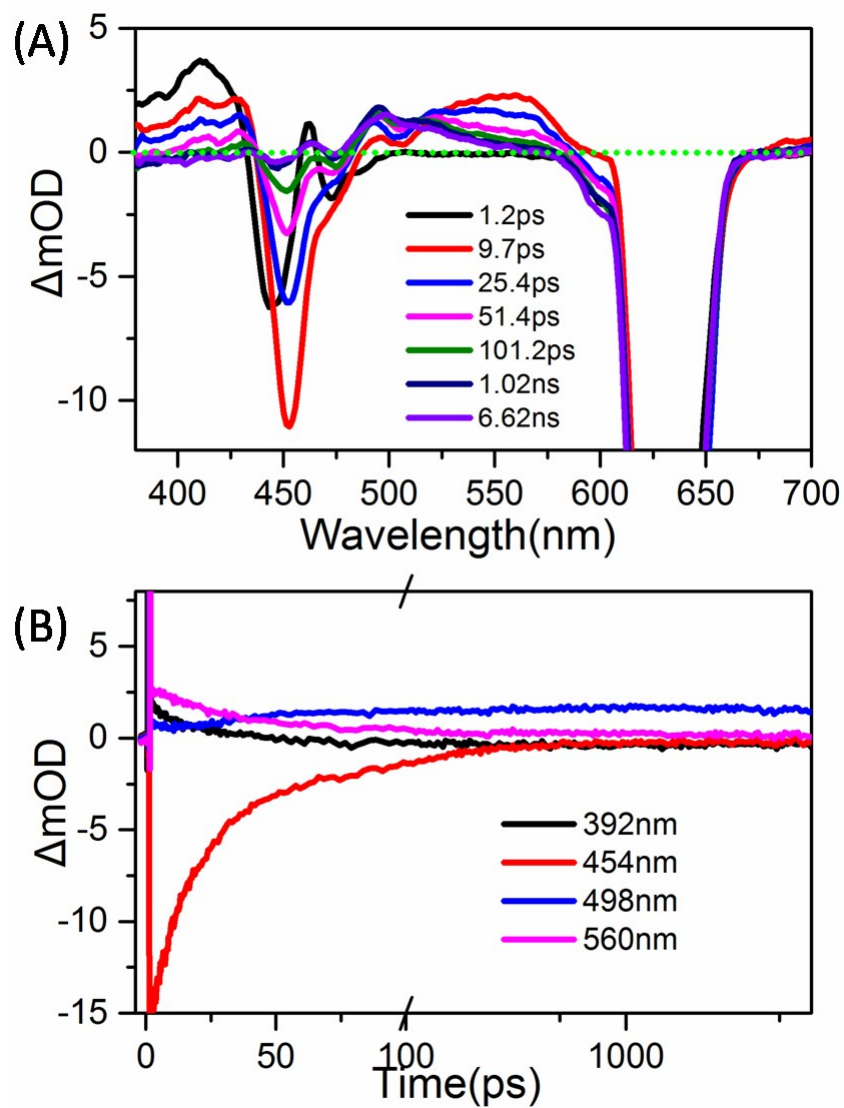


Fig. S8 (A) TA spectra of the mixture of PdTPTBP and DPhTc NP following excitation of PdTPTBP at 630 nm. (B) Single-wavelength dynamics of the mixture of PdTPTBP and DPhTc NP probed at different wavelengths.

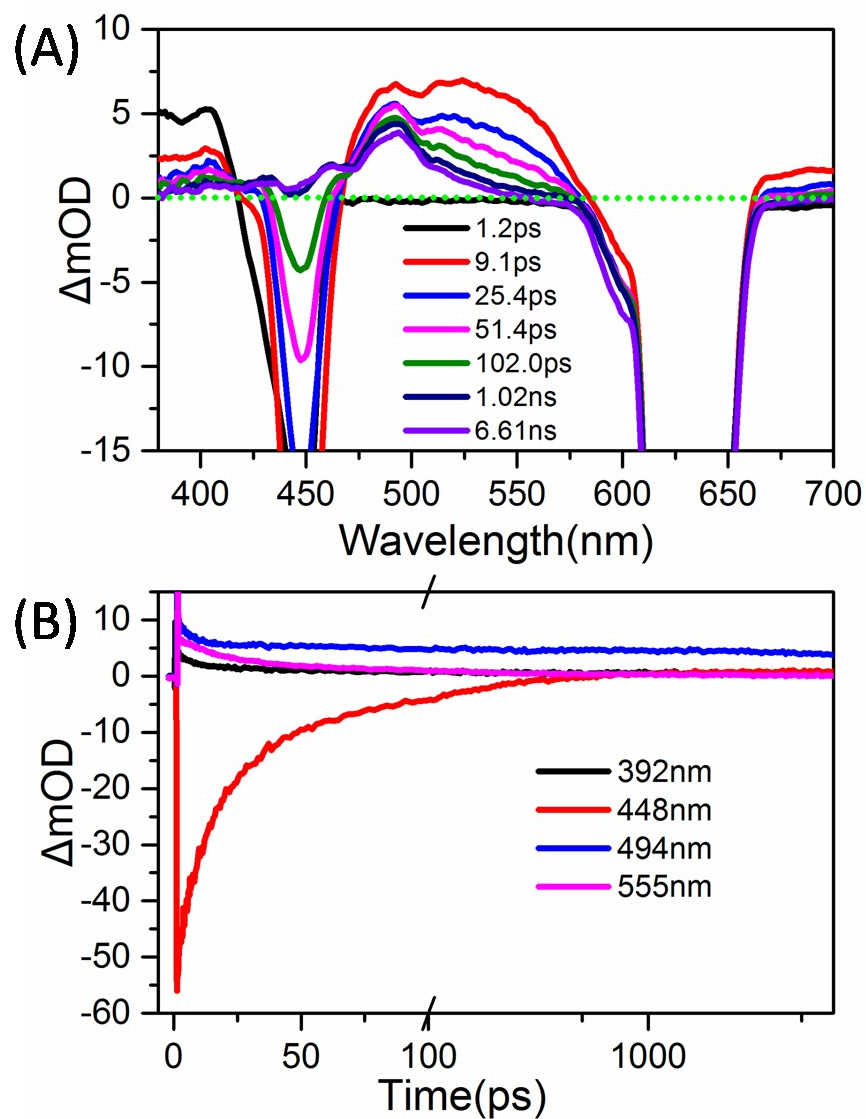


Fig. S9 (A) TA spectra of the mixture of PdTPTBP and DPhTc-COOH NP following excitation of PdTPTBP at 630 nm. (B) Single-wavelength dynamics of the mixture of PdTPTBP and DPhTc-COOH NP probed at different wavelengths.

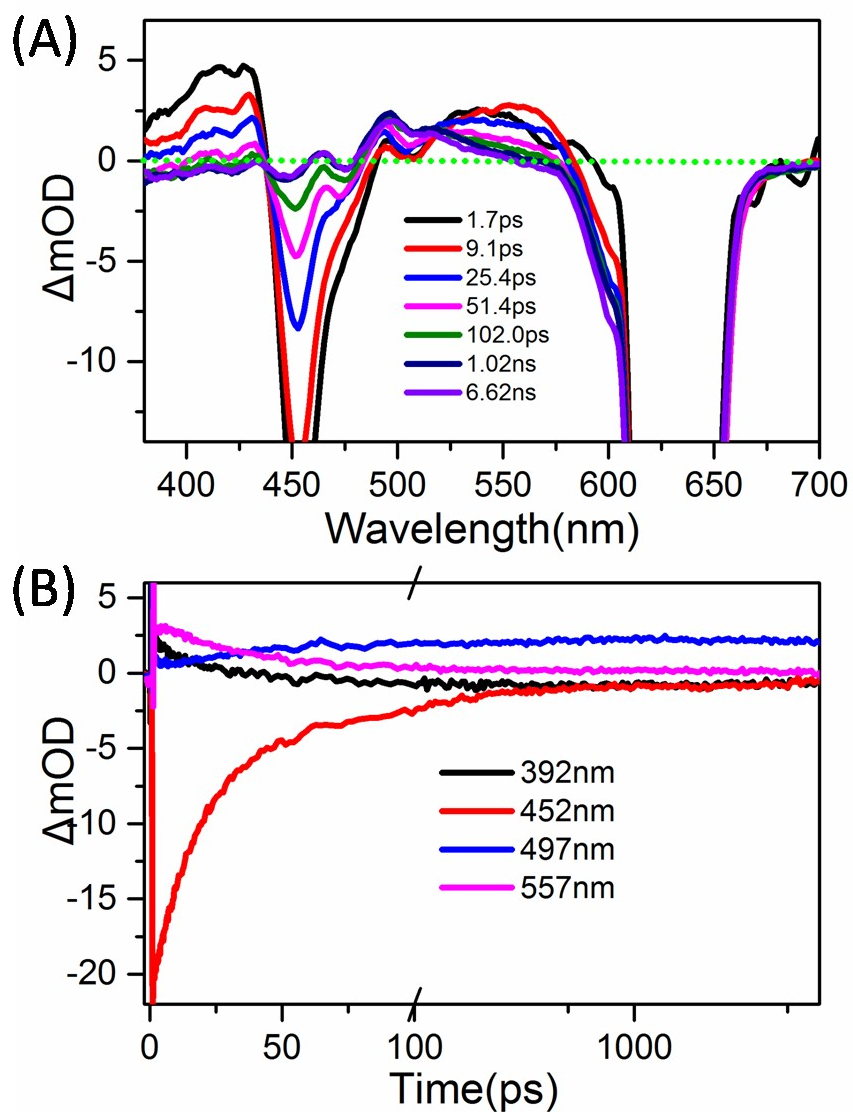


Fig. S10 (A) TA spectra of the mixture of PdTPTBP and DPhTc-(COOH)₂ NP following excitation of PdTPTBP at 630 nm. (B) Single-wavelength dynamics of the mixture of PdTPTBP and DPhTc-(COOH)₂ NP probed at different wavelengths.

6. Comparison of TA spectra between the raw data and the fitting data

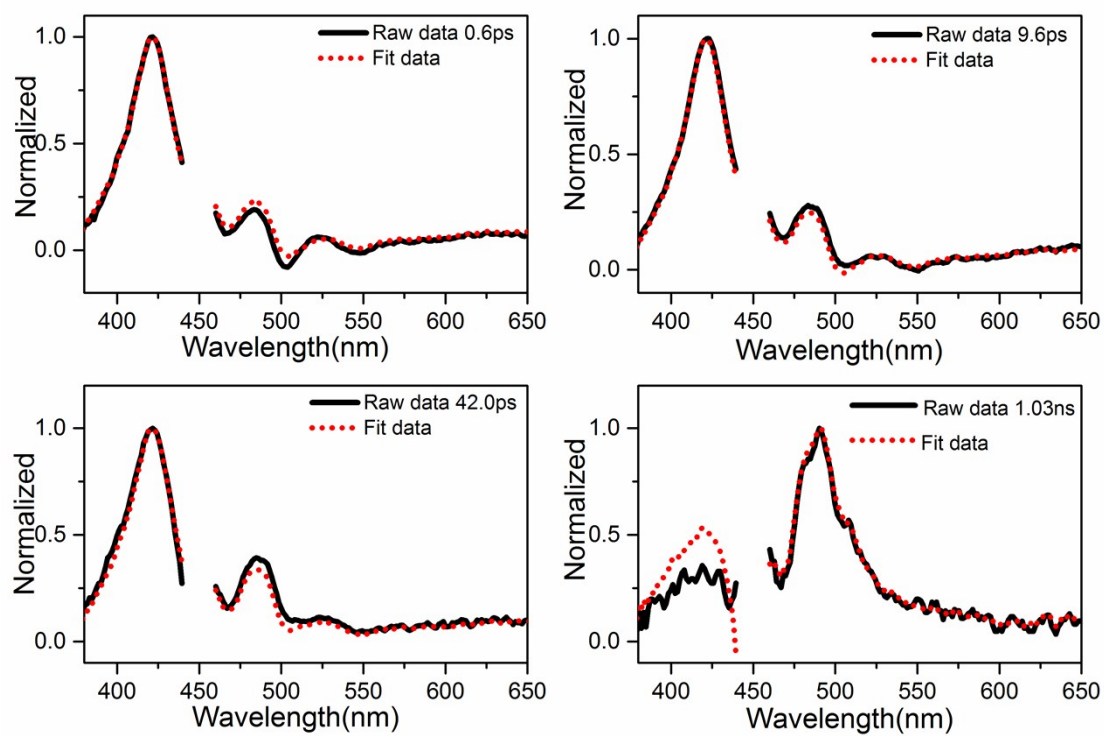


Fig. S11 Comparison of TA spectra of DPhTc NP between the raw data and the fitting data obtained from the global method.

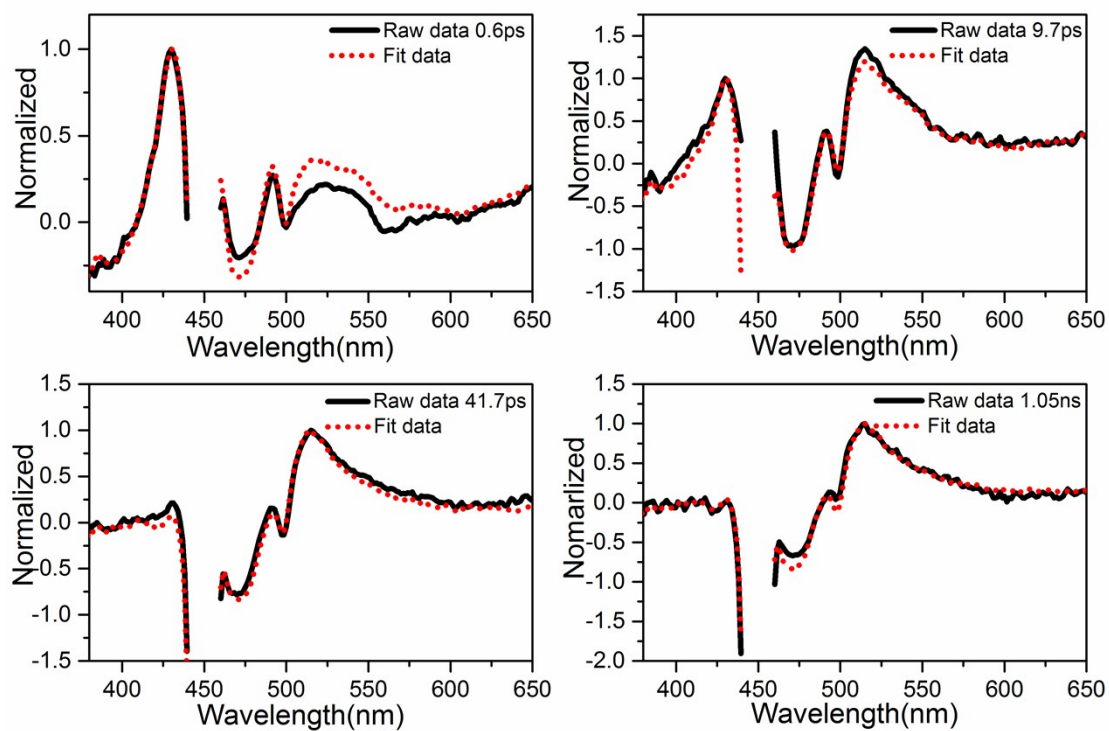


Fig. S12 Comparison of TA spectra of DPhTc-COOH NP between the raw data and the fitting data obtained from the global method.

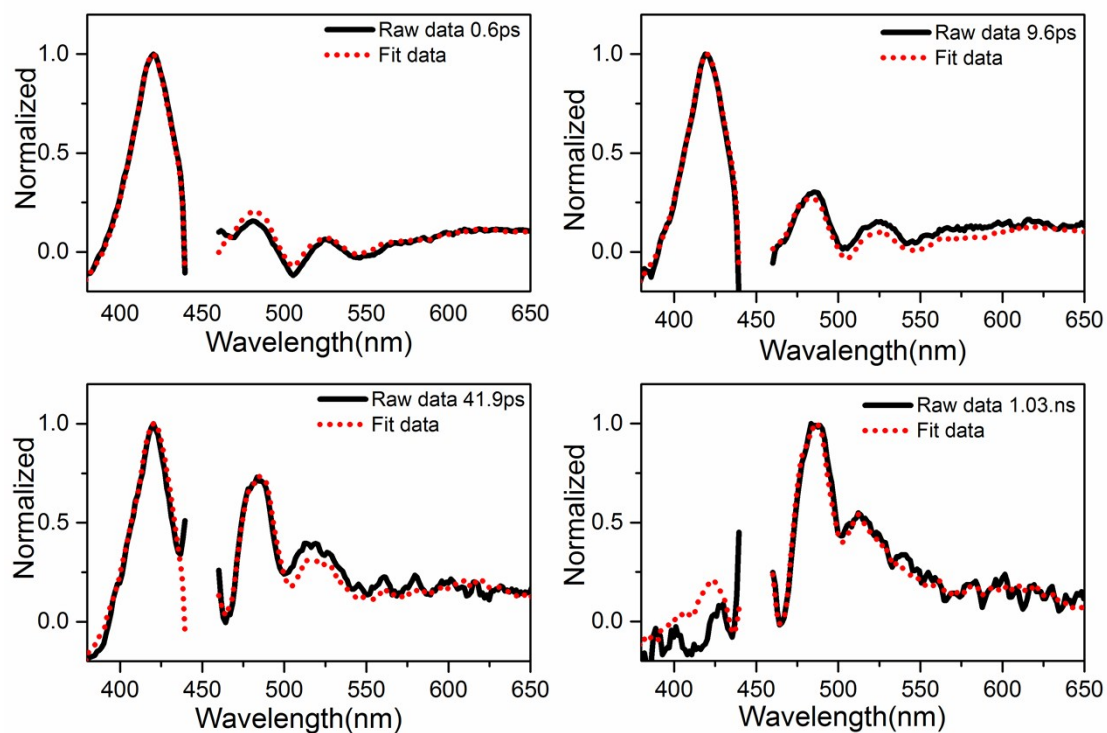


Fig. S13 Comparison of TA spectra of DPhTc-(COOH)₂ NP between the raw data and the fitting data obtained from the global method.

7. Singular value decomposition of *ns*-TA

We use singular value decomposition (SVD) to obtain the dynamics of the $^1(\text{TT})$ state and the T_1 state or the $^1(\text{T}\cdots\text{T})$ state. For DPhTc NP, an early time spectrum (1.01ns) after photoexcitation was chosen as the basic spectrum of the $^1(\text{TT})$ state according to the *fs*-TA spectra. Accordingly, the spectrum monitored at 217.6 ns was chosen as the basic spectrum of the T_1 state. Then these two spectra were used to extract the dynamics of the $^1(\text{TT})$ state and the T_1 state (Figure 7 in the main text). Similarly, the spectra monitored at 1 ns and 131.7 ns were used as the basic spectra of the $^1(\text{TT})$ state and the $^1(\text{T}\cdots\text{T})$ state, respectively.

8. Triplet yield determination

Because the spectra of $^1(TT)$ obtained from SF are all similar with the triplet spectra from the sensitization experiment, we can estimated the triplet quantum yields through the spectra of $^1(TT)$ in these three kinds of nanoparticles using a ground-state bleaching method as the literatures reported.⁶⁻⁸ An early time trace (0.53ps) after photoexcitation for DPhTc NP, the S_1 concentration is assumed C_1 , whereas the $^1(TT)$ concentration remains nearly 0. At initial time, the S_0 concentration is C_0 .

$$\Delta C(0.53ps) = S_1(0.53ps) - S_0 = (C_0 - C_1 - 0) - C_0 = -C_1 = -C(S_1) \quad (1)$$

At 374.5ps, S_1 depletes fully as a result of efficient SF and $^1(TT)$ generates according to global analysis result (Figure 6 of the main text).

$$\Delta C(374.5ps) = (C_0 - 0 - C(^1(TT))) - C_0 = -C(^1(TT)) \quad (2)$$

Therefore, the triplet yield of DPhTc NP can be obtained from equation 3.

$$\Phi_{triplet} = C(^1(TT)) / C(S_1) = -\Delta C(374.5ps) / -\Delta C(0.5ps) = GSB(374.5ps) / GSB(0.5ps) \quad (3)$$

As the same to DPhTc NP, the triplet yield of DPhTc-COOH and DPhTc-(COOH)₂ NPs can be obtained from equation 4 and 5.

$$\Phi_{triplet} = GSB(61.3ps) / GSB(0.53ps) \quad (4)$$

$$\Phi_{triplet} = GSB(171.0ps) / GSB(0.53ps) \quad (5)$$

Therefore, the triplet yield is actually proportional to the intensity of the pure GSB. As the transient absorption spectra show the superposition of GSB, S_1 absorption or $^1(TT)$ absorption. Thus, proper subtraction of the scaled GSB spectrum can reproduce the pure S_0 , S_1 , $^1(TT)$ spectra and their respective pure GSB. The specific operation is that only enough ground state absorption is added to the transient

trace in order to remove the extremum at 502nm, 482nm in DPhTc NP, 496nm, 474nm in DPhTc-COOH NP and 503nm, 467nm in DPhTc-(COOH)₂ NP due to GSB (Figure S14-S16). Therefore, the SF efficiencies and triplet yields can be determined ($75 \pm 10\%$ for DPhTc, $155 \pm 10\%$ for DPhTc-COOH NP, $93 \pm 10\%$ for DPhTc-(COOH)₂ NP).

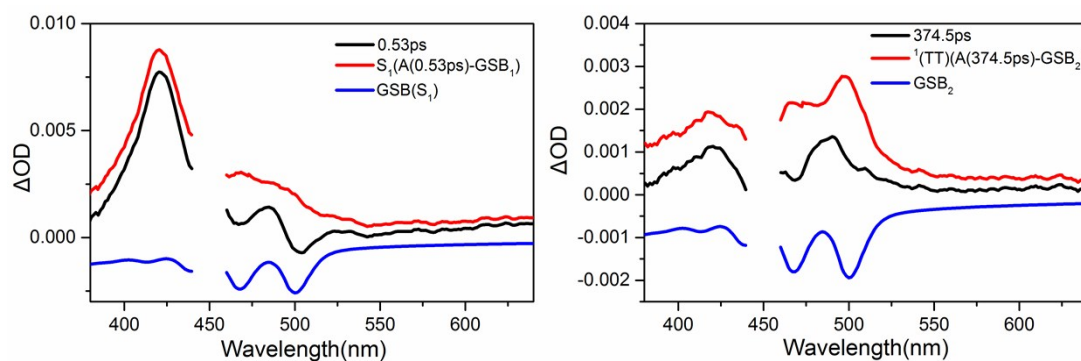


Fig. S14 TA spectra, substraction of the scaled steady state absorption spectra and resulting reconstructed absorption spectra of the pure singlet state (left) and triplet state (right) of the DPhTc NP.

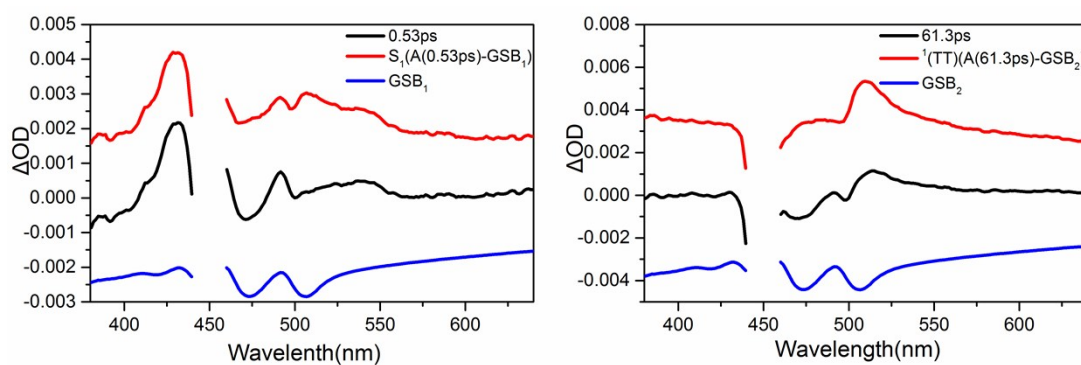


Fig. S15 TA spectra, substraction of the scaled steady state absorption spectra and resulting reconstructed absorption spectra of the pure singlet state (left) and triplet state (right) of the DPhTc-COOH NP.

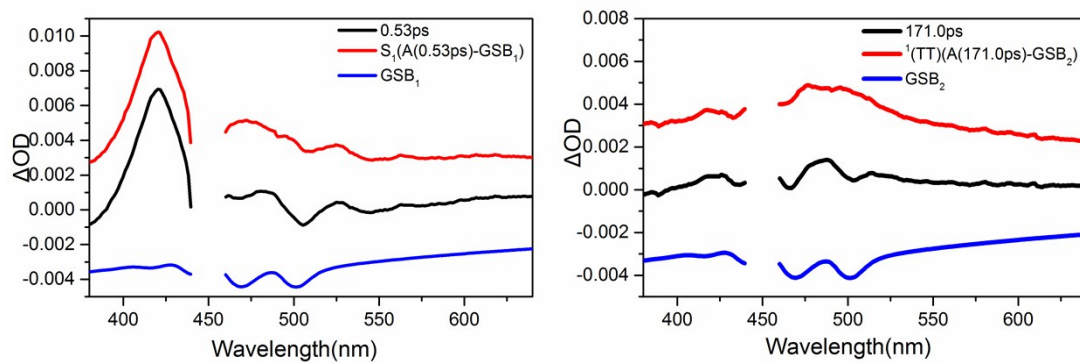


Fig. S16 TA spectra, substraction of the scaled steady state absorption spectra and resulting reconstructed absorption spectra of the pure singlet state (left) and triplet state (right) of the DPhTc-(COOH)₂ NP.

9. Comparison of the arrangement between the minimized packing of DPhTc nanoparticle and its crystal

Single crystal of DPhTc was grown by recrystallization from trichloromethane and methanol (trichloromethane /methanol = 1 / 4.5). The crystallographic data of DPhTc was collected on the Agilent Xcalibur Eos Gemini diffractometer with (Cu) X-ray Source (Cu-K α λ = 1.54184 Å). Experienced absorption was corrected by multiscan method. Using the SADABS program to apply the empirical absorption correction.⁹ The structures were solved by the direct method and refined by the full-matrix least-squares method on F², and all non-hydrogen atoms are refined with anisotropic thermal parameters.¹⁰ The structures of DPhTc has been deposited in the Cambridge Crystallographic Data Centre database (CCDC1965117). All the cell parameters and refinement details were given in the Supporting Information (Table S2). The comparison of the arrangement between the minimized packing of DPhTc and its crystal was shown in Fig. S17 and Table S1.

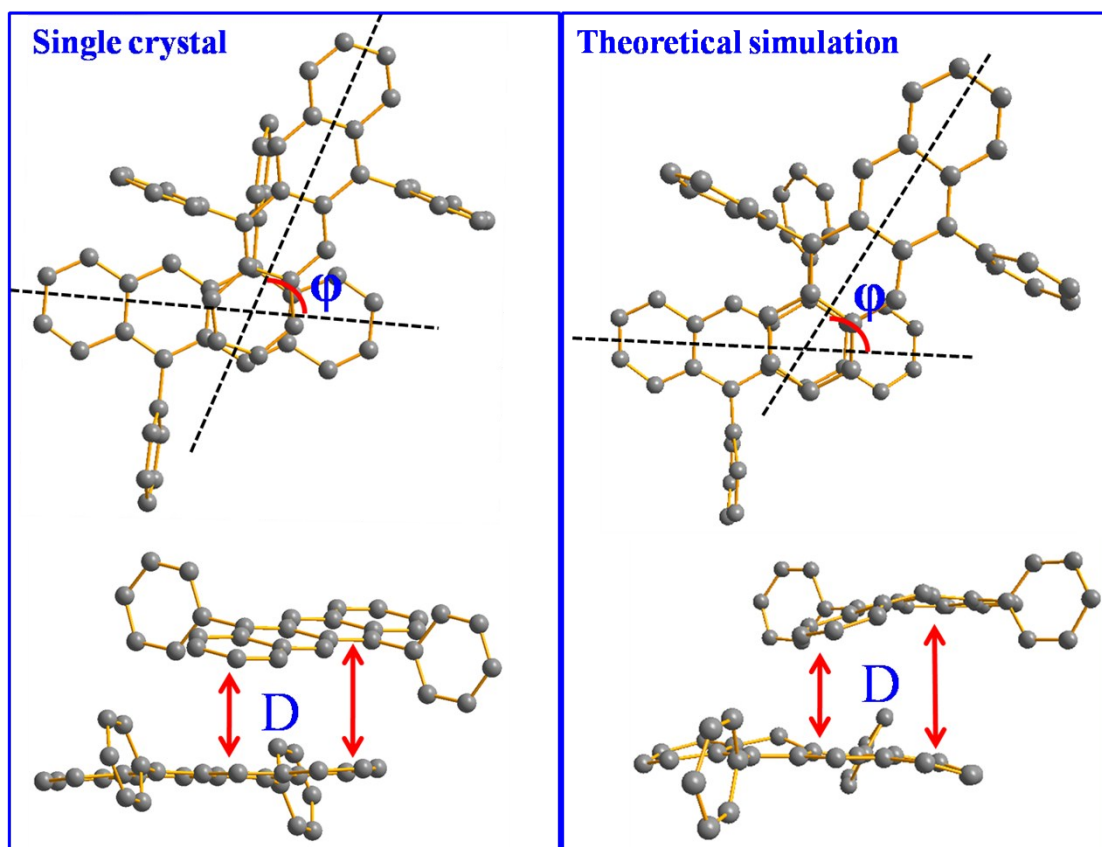


Fig. S17 Comparison of the dimeric structures with strongest interactions between the minimized packing of DPhTc nanoparticle and its crystal.

Table S1 Comparison of the structural parameters of dimeric structures with strongest interactions between the minimized packing of DPhTc nanoparticle and its crystal.

	θ (°)	ϕ (°)	D (Å)
Single crystal	17.6-19.9	70.3	3.9-5.1
Theoretical simulation	19.4-31.8	63.1	4.0-5.5

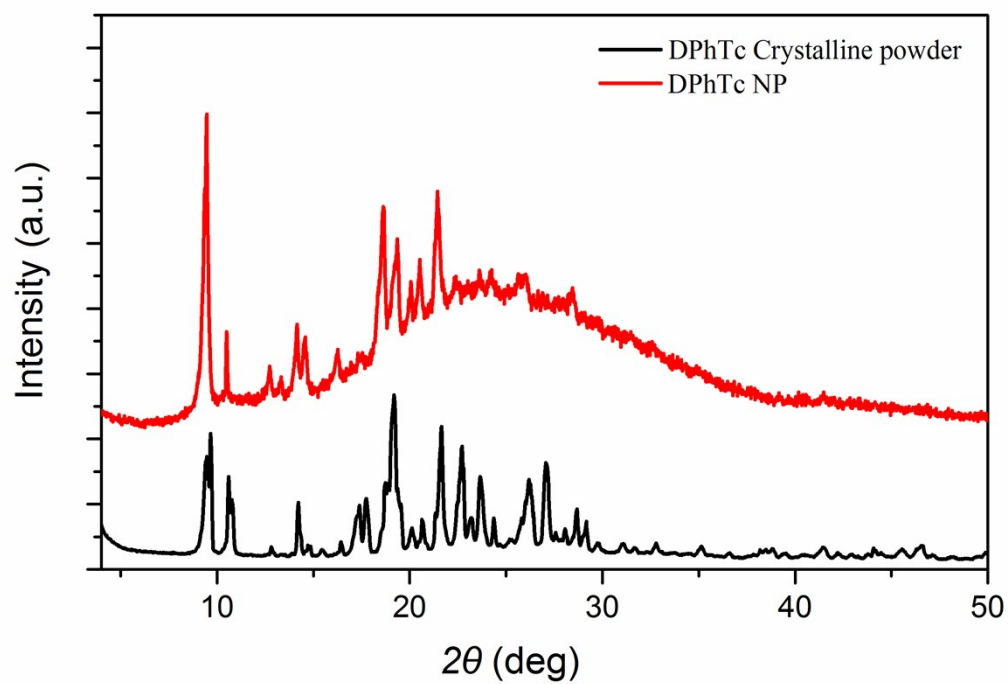


Fig. S18 XRD patterns of crystalline powder and nanoparticle for DPhTc.

Table S2. Crystallographic parameters for molecular DPhTc crystals

	DPhTc
Empirical	C ₆₀ H ₄₀
Formula	760.92
Temperature/K	293.2(2)
Crystal	triclinic
Space	P1
a/Å	9.3181(8)
b/Å	10.9718(7)
c/Å	11.1129(9)
α /°	66.588(7)
β /°	80.267(7)
γ /°	89.605(6)
Volume/Å ³	1025.31(15)
Z	1
ρ calc mg/mm ³	1.232
μ /mm ⁻¹	0.529
F(000)	400
2 θ range for data collection	8.802 to 141.156
Reflections collected	7404
Independent reflections	4862 [R _{int} = 0.0366, R _{sigma} = 0.0480]
Data/restraints/parameters	4862/3/541
Goodness-of-fit on F ²	1.065
Final R indexes [I >= 2 σ (I)]	R ₁ = 0.0474, wR ₂ = 0.1207
Final R indexes [all data]	R ₁ = 0.0734, wR ₂ = 0.1572
Largest diff. peak/hole /e Å ⁻³	0.19/-0.24

10. Simulation of the packing structure of these molecules at the interface of air/water

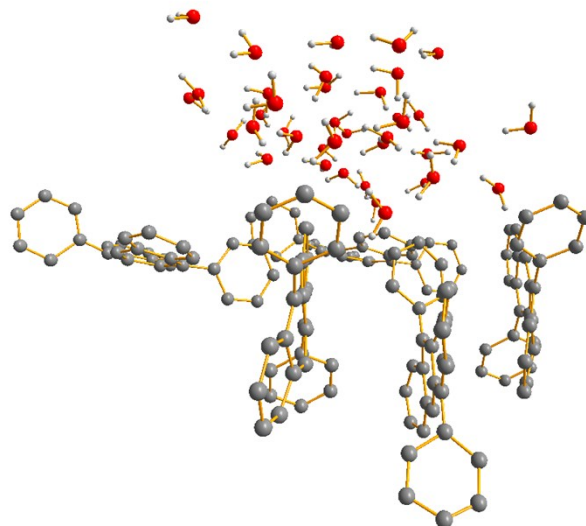


Fig. S19 Simulation of the packing structure of DPhTc at the interface of air/water.

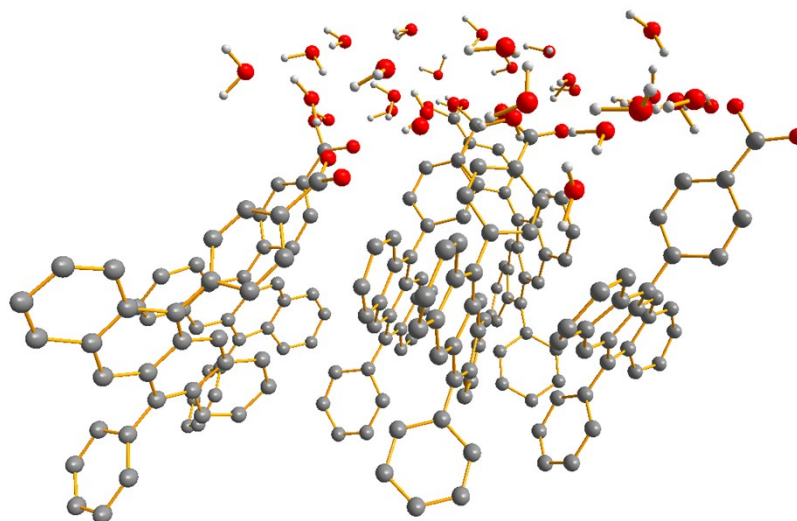


Fig. S20 Simulation of the packing structure of DPhTc-COOH at the interface of air/water.

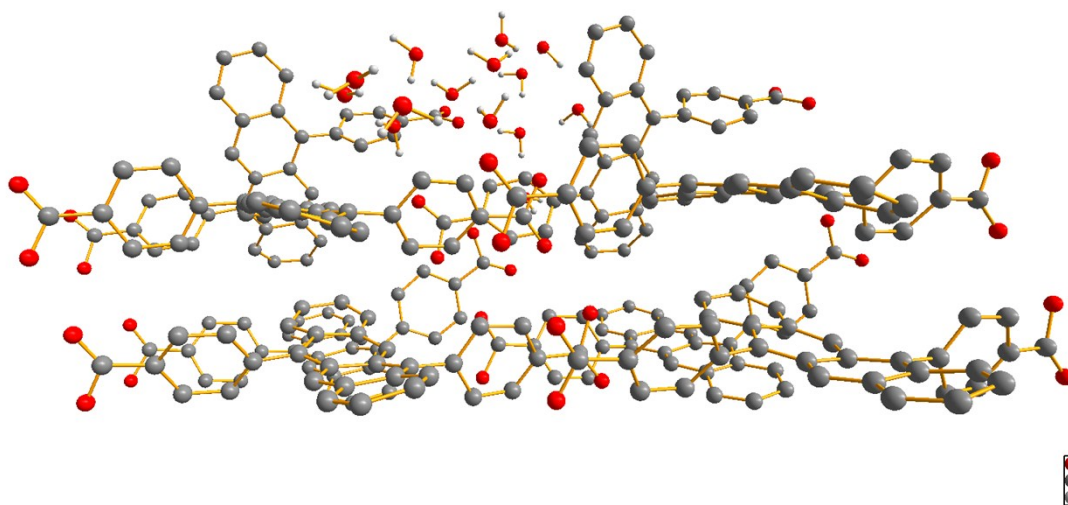


Fig. S21 Simulation of the packing structure of DPhTc-(COOH)₂ at the interface of air/water.

11. Calculation of the splitting energy of the singlet state

We extracted three dimeric structures that are relatively close from the above simulation result for each nanoparticle and calculated their splitting energies of the singlet state at the level of ω b97xd/6-31+G (d) in the Gaussian 09 program package (Table S3-S5, Fig. S22-S24).¹¹ The larger splitting energy of the singlet state indicates the stronger interaction between the adjacent chromophore units.^{12,13}

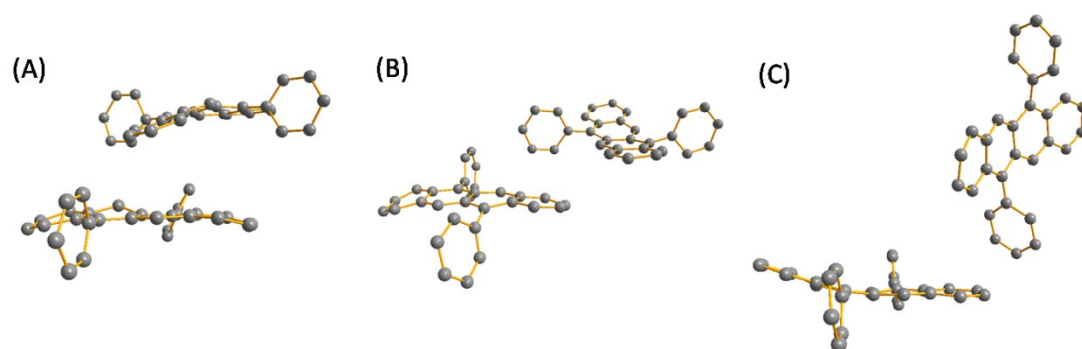


Fig. S22 Three dimeric structures in DPhTc NP extracted from the simulation result.

Table S3 Splitting energies of the singlet state of three dimeric structures in DPhTc NP.

	$S_2(eV)$	$S_1(eV)$	$\Delta E(eV)$
A	2.3720	2.2914	0.0806
B	2.4344	2.3681	0.0663
C	2.3122	2.2607	0.0515

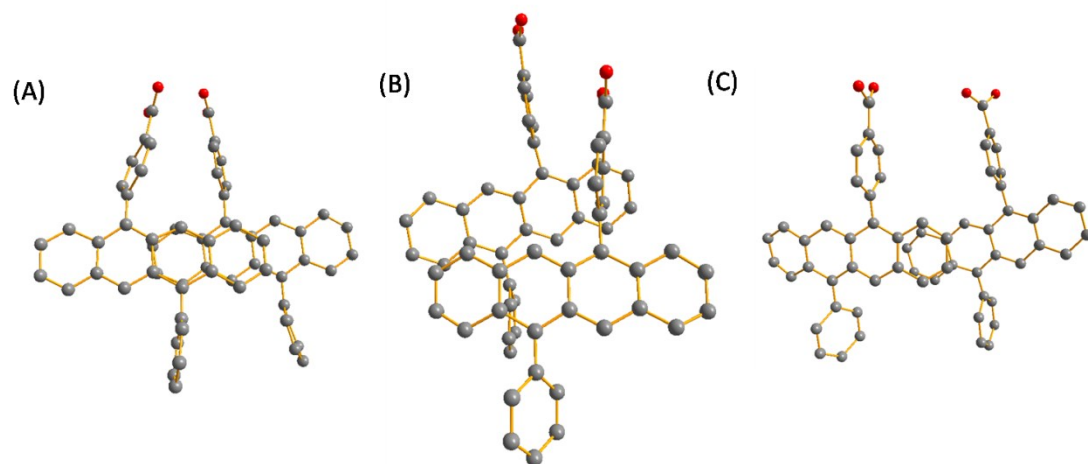


Fig. S23 Three dimeric structures in DPhTc-COOH NP extracted from the simulation result.

Table S4 Splitting energies of the singlet state of three dimeric structures in DPhTc-COOH NP.

	$S_2(eV)$	$S_1(eV)$	$\Delta E(eV)$
A	2.4254	2.1382	0.2872
B	2.4519	2.3515	0.1004
C	2.4934	2.3495	0.1439

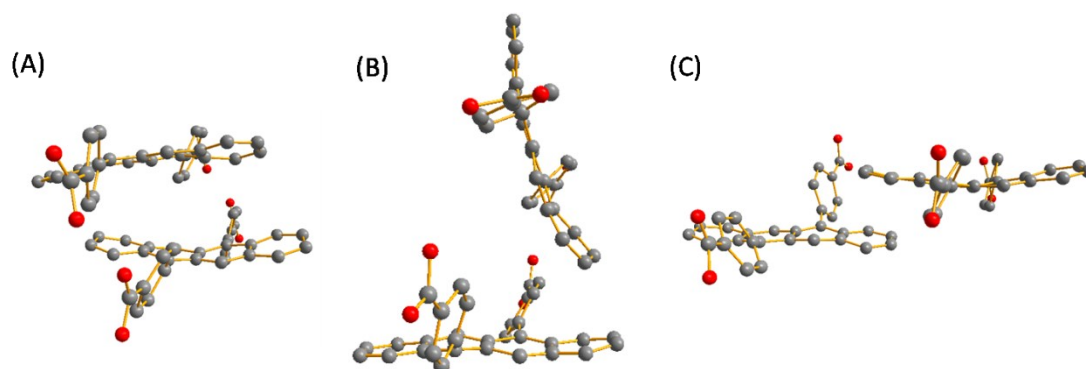


Fig. S24 Three dimeric structures in DPhTc-(COOH)₂ NP extracted from the simulation result.

Table S5 Splitting energies of the singlet state of three dimeric structures in DPhTc-(COOH)₂ NP.

	$S_2(eV)$	$S_1(eV)$	$\Delta E(eV)$
A	2.4447	2.2648	0.1799
B	2.3115	2.2599	0.0516
C	2.4452	2.3056	0.1396

12. ^1H NMR and MALDI-TOF spectra of new compounds

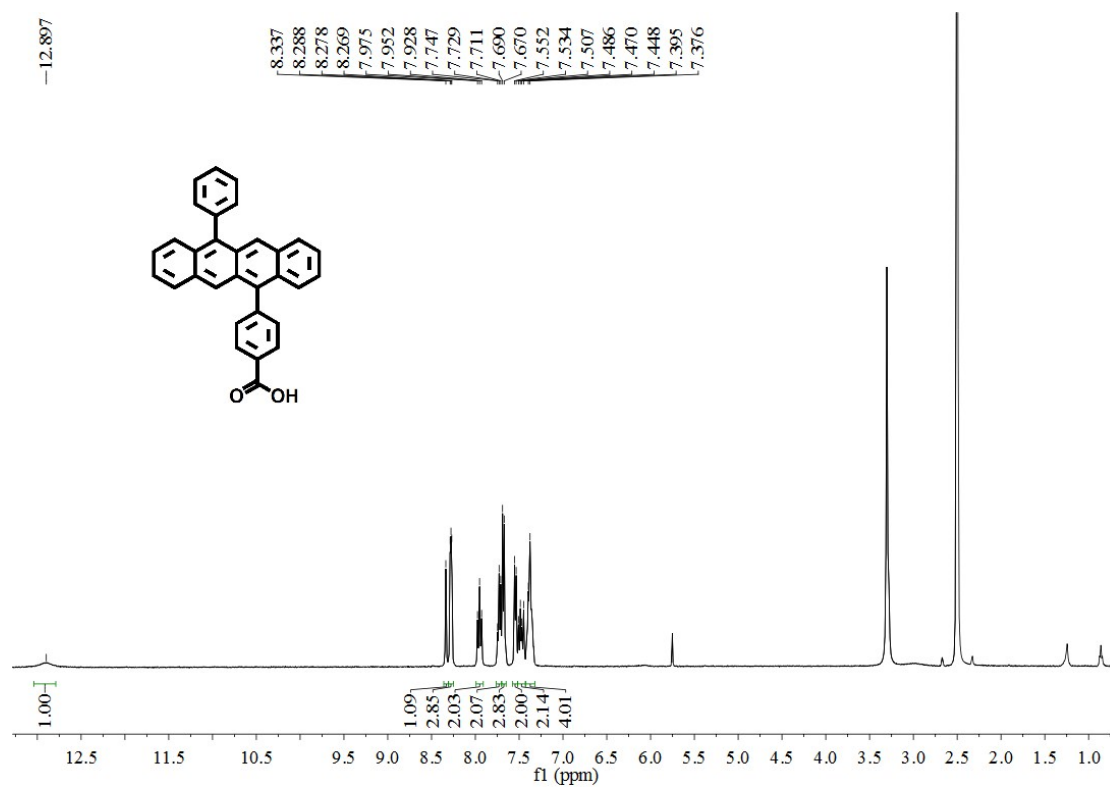


Fig. S25 ^1H NMR spectrum of DPhTc-COOH.

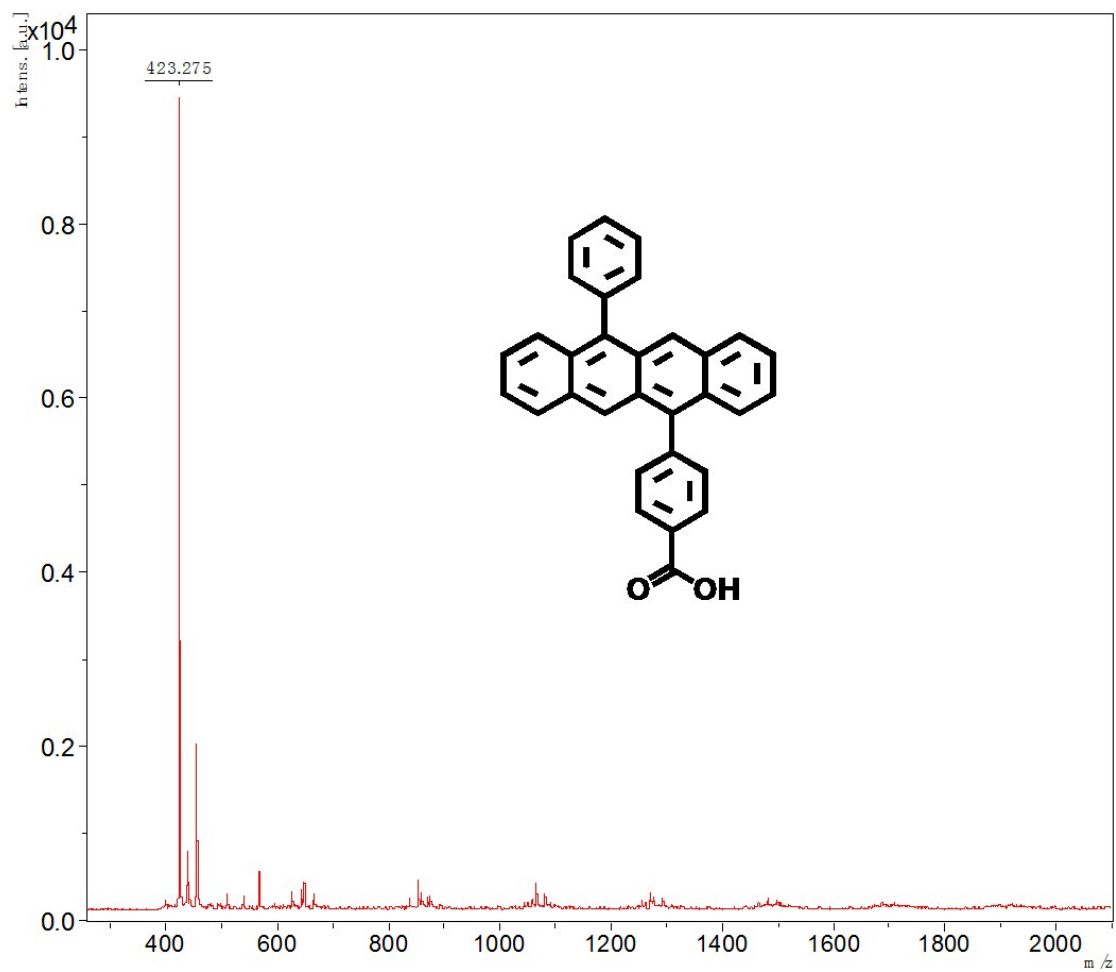


Fig. S26 MALDI-TOF spectrum of DPhTc-COOH.

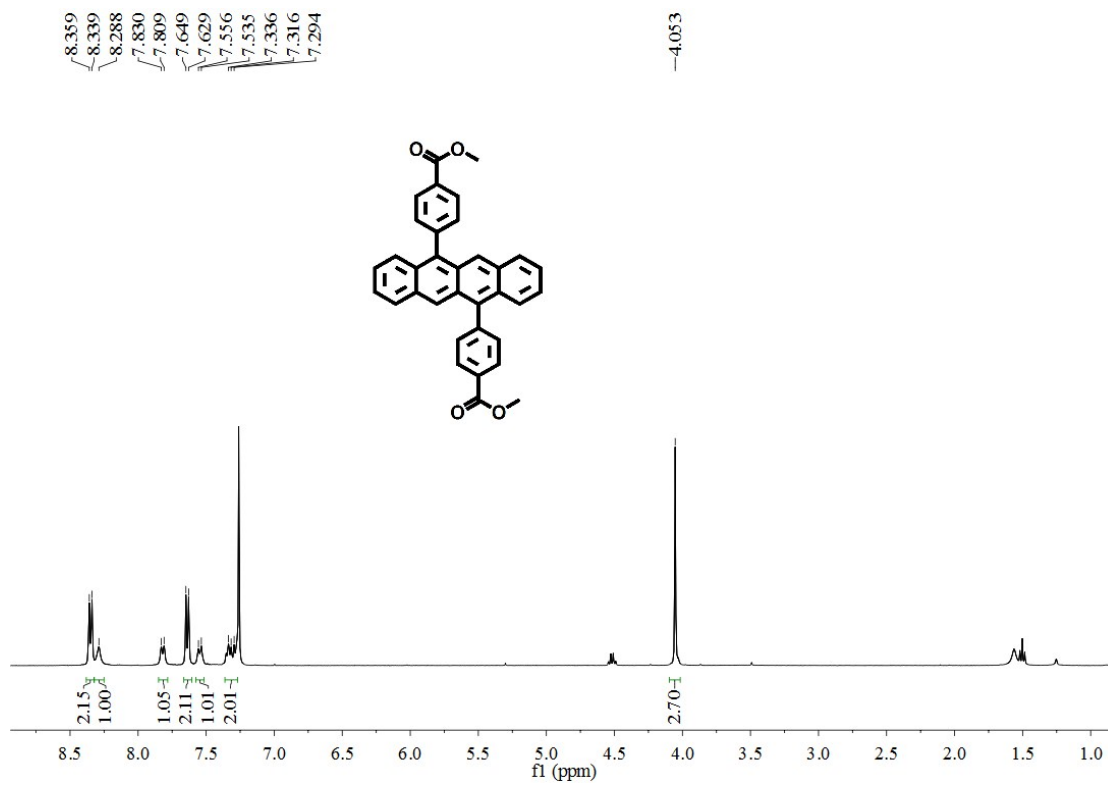


Fig. S27 ¹H NMR spectrum of compound 4.

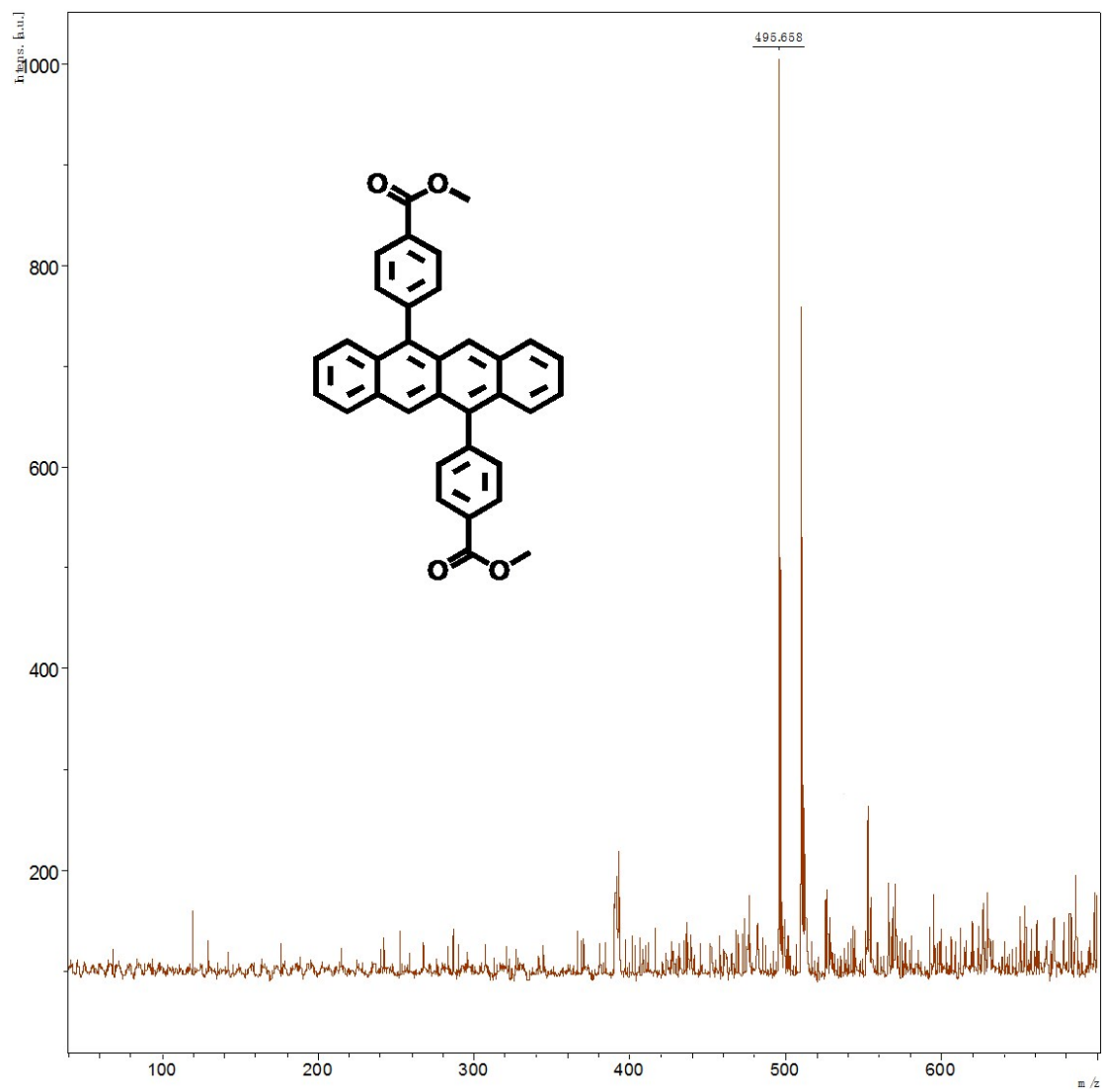


Fig. S28 MALDI-TOF spectrum of compound **4**.

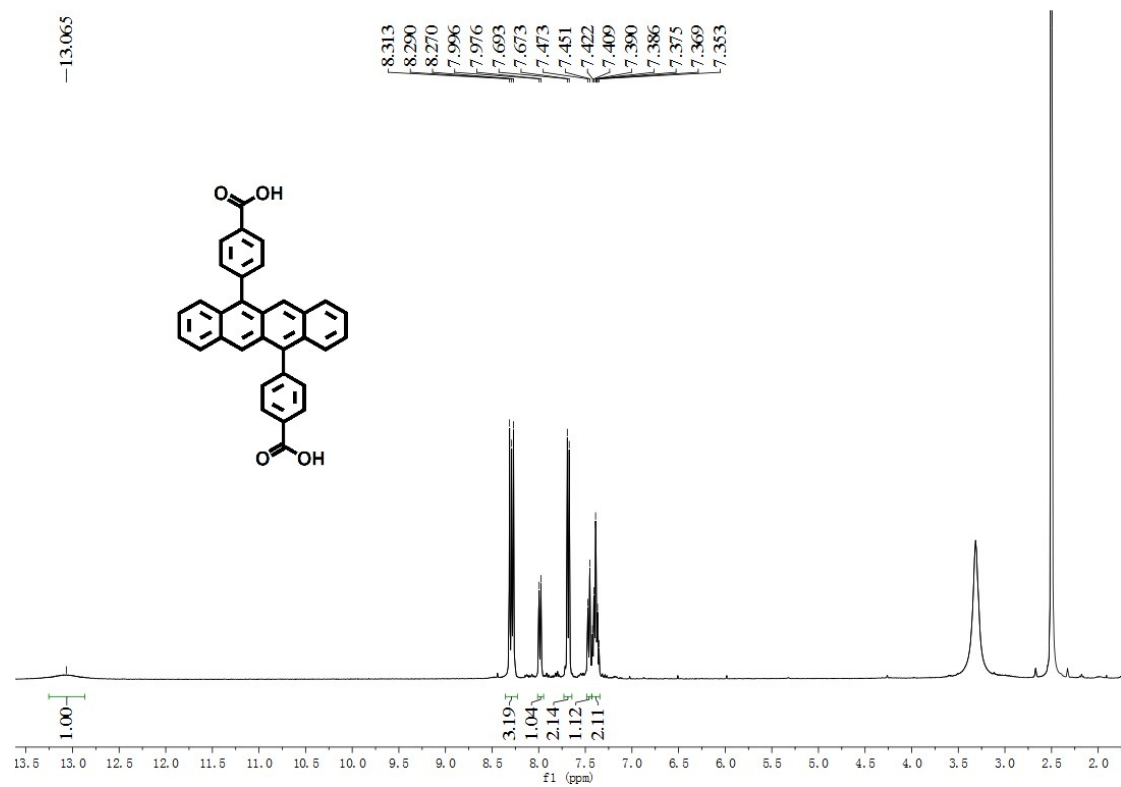


Fig. S29 MALDI-TOF spectrum of DPhTc-(COOH)₂.

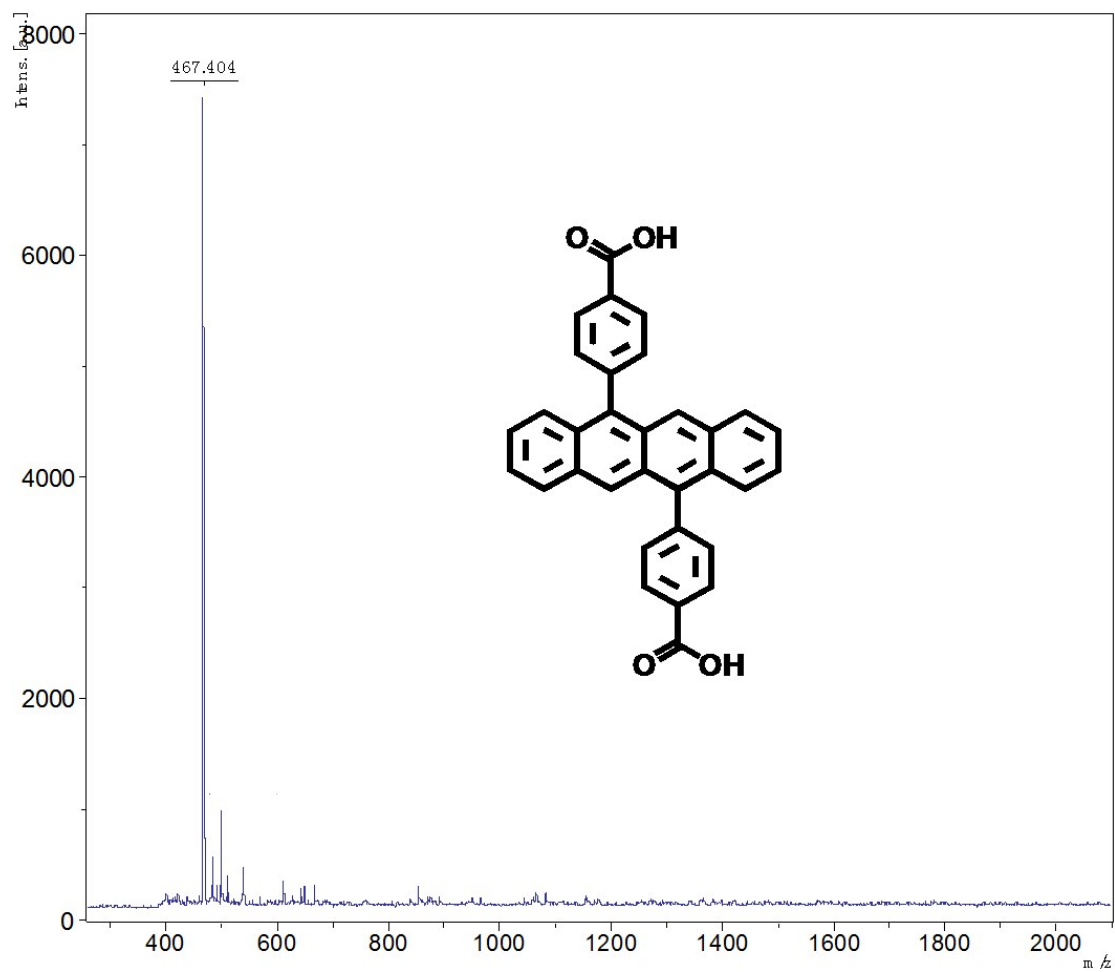


Fig. S30 MALDI-TOF spectrum of DPhTc-(COOH)₂.

REFERENCES

- [1] R. Tao, J. Zhao, F. Zhong, C. Zhang, W. Yang and K. Xu, *Chem. Commun.*, 2015, **51**, 12403-12406.
- [2] X. Cui, J. Zhao, P. Yang and J. Sun, *Chem. Commun.*, 2013, **49**, 10221-10223.
- [3] S. T. Roberts, R. E. Mcanally, J. N. Mastron, D. H. Webber, M. T. Whited, R. L. Brutchey, M. E. Thompson and S. E. Bradforth, *J. Am. Chem. Soc.*, 2012, **134**, 6388-6400.
- [4] J. N. Mastron, S. T. Roberts, R. E. Mcanally, M. E. Thompson and S. E. Bradforth, *J. Phys. Chem. A*, 2013, **117**, 15519-15526.
- [5] C. Burgdorff, T. Kircher and H. G. Löhmansröben, *Spectrochim. Acta. A*, 1988, **44**, 1137-1141.
- [6] Z. Tang, S. Zhou, X. Wang, H. Liu, X. Yan, S. Liu, X. Lu and X. Li, *J. Mater. Chem. C*, 2019, **7**, 11090-11098
- [7] Y. Wu, K. Liu, H. Liu, Y. Zhang, H. Zhang, J. Yao, H. Fu, *J. Phys. Chem. Lett.*, 2014, **5**, 3451-3455.
- [8] E. A. Margulies, Y. L. Wu, P. Gawel, S. A. Miller, L. E. Shoer, R. D. Schaller, F. Diederich, M. R. Wasielewski, *Angew. Chem. Int. Ed.*, 2015, **54**, 8679-5683.
- [9] S. Parkin, H. J. Hope, *App. Crystallogr.*, 1998, **31**, 945-923.
- [10] G. M. Sheldrick, *Acta. Crystallogr. C*, A 2015, **71**, 3-8.
- [11] M. Frisch, G. Trucks, H. Schlegel, G. Scuseria, M. Robb, J. Cheeseman, G. Scalmani, V. Barone, B. Mennucci and G. Petersson, Gaussian Inc., Wallingford, CT, 2010.

[12] B. S. Basel, C. Hetzer, J. Zirzmeier, D. Thiel, R. Guldi, F. Hampel, A. Kahnt, T.

Clark, D. M. Guldi and R. R. Tykwinski, *Chem. Sci.*, 2019, **10**, 3854-3863

[13] P. J. Vallett, J. L. Snyder and N. H. Damrauer, *J. Phys. Chem. A*, 2013, **117**,

10824-10838.